

SYNTHESIS AND CHARACTERIZATION OF POLY[3-(2',5'-DIHEPTYLOXY-PHENYL)THIOPHENE] FOR USE IN PHOTOELECTROCHEMICAL CELLS

Assefa Sergawie, Shimelis Admassie*, Wendimagegn Mammo, Teketel Yohannes and Theodros Solomon

Department of Chemistry, Addis Ababa University, P.O. Box 1176, Addis Ababa, Ethiopia

(Received August 17, 2006; revised December 13)

ABSTRACT. Poly[3-(2',5'-diheptyloxyphenyl)thiophene], PDHOPT, has been prepared electrochemically from its monomer for solar cell application. PDHOPT exhibits a band gap of 2.1 eV. The redox properties of PDHOPT were characterized using cyclic voltammetry. The estimated energy levels of the highest occupied molecular orbital (HOMO) and the lowest unoccupied molecular orbital (LUMO) are -5.3 eV and -3.2 eV, respectively. PDHOPT sensitizes nanocrystalline titanium dioxide (nc-TiO₂) in liquid-state photoelectrochemical cells. Devices where the photoactive electrode consists of nc-TiO₂/PDHOPT composite film show improved performance over those that consist of only PDHOPT. Devices made of TiO₂/PDHOPT composite film produced an open-circuit voltage of 0.52 V, a short-circuit current of 29 $\mu\text{A}/\text{cm}^2$, and a fill factor of 0.54 when illuminated with white light intensity of 80 mW/cm².

KEY WORDS: Liquid-state photoelectrochemical cell, Nanocrystalline titanium dioxide, PDHOPT, I₃/I redox couple

INTRODUCTION

Dye-sensitized photoelectrochemical cells (DSSC) are considered low cost alternatives to the inorganic photovoltaic cells [1]. The cells are composed of nanocrystalline TiO₂ film deposited on a transparent conductive electrode (anode), a dye, chemically anchored on TiO₂ nanoparticles, an electrolyte bearing the I₃/I redox couple and a platinized transparent conductive electrode (cathode). Following light absorption by the dye, electrons are excited from the highest occupied molecular orbital (HOMO) to the lowest unoccupied molecular orbital (LUMO) followed by relaxation through electron loss to the semiconductor. The dye cation is neutralized by the chemical reaction with the redox couple in the electrolyte solution which in turn gains an electron from a counter electrode, making the process regenerative for the conversion of incident light to electric current. For effective electron transfer to the TiO₂, the energy level of the LUMO of the dye (electron donor) should be higher than the conduction band (CB) edge of the semiconductor (electron acceptor) and the HOMO should lie above the valence band (VB) of the semiconductor but below the electrochemical potential of the redox couple. The power conversion efficiency of such cells has reached 10.4 % [2]. Despite their high power conversion efficiencies, their commercial applications are limited due to problems like leakage of the electrolyte and the degradation of both the electrolyte [3] and the dye [4]. Various studies with different approaches have been carried out to alleviate the problems associated with liquid-state DSSCs. These include replacement of the liquid electrolyte by a polymer electrolyte [5], introduction of gelifiers [6] and nanocomposite organic-inorganic gel [7] into the electrolyte and replacement of the dye by a semiconducting polymer [8-10].

The donor-acceptor system of organic solar cells has been studied in solid-state organic photovoltaic cells based on conjugated polymers. Heterojunctions based on blends of conjugated polymers (electron donors following photoexcitation) with fullerene and its derivative (electron acceptors) are the best-studied devices and they have yielded the highest power conversion efficiencies reaching around 5 % [11-13]. In such photovoltaic cells, the

*Corresponding author. E-mail: shimadm@chem.aau.edu.et, shimadm@yahoo.com

semiconducting polymer takes care of the absorption of the sunlight, charge injection into the fullerene or its derivative and the transport of holes after charge separation. Besides these fully organic photovoltaic devices, semiconducting polymers can also be used in combination with inorganic semiconductors such as TiO₂, ZnO and CuInSe₂ [14-19]. In these hybrid organic/inorganic devices, the good electron accepting and conducting properties of the inorganic semiconductors can, in principle, be combined with cheap, solution processing of the semiconducting polymers. The disadvantages of many of these systems are the low hole-mobility in semiconducting conjugated polymers compared with the electron-mobility in inorganic semiconductors [20] and the incomplete filling of the nanopores of the inorganic semiconductor by the polymers [19].

The sensitization of inorganic semiconductors by conjugated polymers [8, 10] has been investigated in liquid-state PECs where the hole-mobility is facilitated by the redox couple. Devising DSSCs with conducting polymers requires preparation of suitable polymers with appropriate band gaps, band positions (with respect to the inorganic semiconductor) and method of deposition. To this end, we present a photoelectrochemical cell where the dye is replaced by the polymer, poly[3-(2',5'-diheptyloxyphenyl)thiophene], PDHOPT, and the Pt counter electrode is replaced by electropolymerized poly[3,4-ethylenedioxythiophene], PEDOT, that is less costly [21]. PDHOPT, electrochemically grown on nc-TiO₂ coated ITO-glass improves the filling of the nanopores of TiO₂ by the polymer.

EXPERIMENTAL

Monomer synthesis

1,4-Diheptyloxybenzene (**3**)

The synthesis of the monomer used in electropolymerization was recently published but without details [22]. We present in the following the full set of synthetic details. To a mixture of hydroquinone (**1**) (5 g, 45.4 mmol), K₂CO₃ (20 g) and DMF (60 mL) at 100 °C was added dropwise 1-bromoheptane (**2**) (18 g, 100.6 mmol) and was heated overnight. The mixture was filtered while still hot and the filtrate was cooled to room temperature. The resulting precipitate was collected and was washed with 1 M NaOH, and water, and recrystallized from MeOH to afford compound **3** (9.09 g, 65 %) as shining white crystals. Mp 57.4-57.8 °C. HRMS: calcd. for C₂₀H₃₄O₂ 306.2559 found 306.2505. EIMS *m/z* (rel. int.): 306 (26), 208 (13), 110 (100), 57 (18). ¹H NMR (CDCl₃, 400 MHz): δ 6.82 (4H, *s*, 4 x Ar-H), 3.89 (4H, *t*, 2 x OCH₂), 1.75 (4H, *m*, 2 x CH₂), 1.26-1.48 (16H, 8 x CH₂), 0.89 (12H, 2 x CH₃).

1-Bromo-2,5-diheptyloxybenzene (**4**)

To a solution of compound **3** (8.4 g, 27.4 mmol) in DMF (100 mL) and CHCl₃ (50 mL) was added a solution of NBS (4.89 g, 27.5 mmol) in DMF (40 mL). After the addition was complete, the mixture was stirred overnight. It was then acidified with 2 M HCl, and extracted with CHCl₃. The CHCl₃ extract was washed with water, dried over Na₂SO₄ and the solvent was removed to afford a brownish oil. The oil was chromatographed over silica gel using pentane: CH₂Cl₂ as eluent to afford compound **4** (7.5 g, 71 %) as a colorless oil. HRMS: calcd. for C₂₀H₃₃O₂Br 384.1664, found 384.1666. EIMS *m/z* (rel. int.): 386 M⁺+2 (17), 384 M⁺ (17), 288 (21), 286 (22), 190 (97), 188 (100), 110 (9), 57 (49). ¹H NMR (CDCl₃, 400 MHz): δ 7.11 (1H, *d*, *J* = 2.8 Hz, H-6), 6.82 (1H, *d*, *J* = 8.8 Hz, H-3), 6.78 (1H, *dd*, *J* = 8.8, 2.8 Hz, H-4), 3.95 (2H, *t*, *J* = 6.4 Hz, OCH₂), 3.88 (2H, *t*, *J* = 6.4 Hz, OCH₂), 1.77 (4H, *m*, 2 x CH₂), 1.27-1.54 (16H, *m*, 8 x CH₂), 0.89 (6H, *t*, 2 x CH₃).

3-(2', 5'-Diheptyloxyphenyl)thiophene (6)

A mixture of compound **4** (7.3 g, 18.96 mmol) and Pd(PPh₃)₄ (0.6 g) in dimethoxy ethane (150 mL) was stirred at room temperature for 10 min and to it was added 3-thiophene boronic acid (**5**) (4.8 g, 37.5 mmol) followed by 1 M NaHCO₃ (100 mL). It was then heated under reflux for 3 h, cooled and filtered. The filtrate was extracted with pentane and the pentane extract was washed with water, dried over anh. Na₂SO₄ and the solvent was removed to afford a dark colored residue. This was taken-up in pentane, filtered and the solvent was removed. The resulting oil was crystallized from MeOH:ether to afford compound **6** (6.54 g, 89 %) as a white solid. Mp 35.8-36.1 °C. HRMS: calcd for C₂₄H₃₆O₂S 388.2436, found 388.2438. EIMS *m/z* (rel. int.): 388 (61), 290 (25), 192 (100), 163 (6). ¹H NMR (CDCl₃, 400 MHz): δ 7.65 (1H, *dd*, *J* = 3.2, 1.2 Hz, H-2), 7.45 (1H, *dd*, *J* = 4.8, 1.2 Hz, H-5), 7.32 (1H, *dd*, *J* = 4.8, 3.2 Hz, H-4), 7.07 (1H, *d*, *J* = 2.8 Hz, H-6'), 6.88 (1H, *d*, *J* = 8.8 Hz, H-3'), 6.78 (1H, *dd*, *J* = 8.8, 2.8 Hz, H-4'), 3.93 (4H, *dd*, *J* = 12, 6.4, 2 x OCH₂), 1.77 (4H, *m*, 2 x CH₂), 1.26-1.48 (16H, 8 x CH₂), 0.89 (3H, *t*, *J* = 6.4, CH₃), 0.88 (3H, *t*, *J* = 6.4, CH₃). ¹³C NMR (CDCl₃, 125.7 MHz): δ 53.3, 150.4, 138.5, 128.7, 126.2, 124.4, 123.4, 116.4, 114.1, 113.6, 69.5, 68.8, 32.0, 31.9, 29.6, 29.6, 29.3, 29.2, 26.3, 26.2, 22.8, 22.8, 14.3, 14.3.

Electrochemical synthesis of PDHOPT

The electrochemical synthesis of PDHOPT was carried out from its monomer, 3-(2',5'-diheptyloxyphenyl)thiophene (**6**), DHOPT, using cyclic voltammetry on different substrates (ITO-glass, nc-TiO₂ coated ITO-glass and glassy carbon) in a three-electrode cell. The chemical polymerization of DHOPT (**6**) using FeCl₃ as oxidant was reported earlier [22]. The glassy carbon disc electrode (3 mm in diameter) was cleaned with Al₂O₃ powder (0.05 micron) prior to polymerization. The electrolyte solution contained 1 mM of the monomer in 0.1 M LiClO₄/CH₃CN solution. Ag/AgCl and Pt wire were used as quasi-reference electrode and counter electrode respectively. The solution was purged with argon for 15 min and remained under argon through out the polymerization process. The cyclic voltammogram of the polymer was recorded in 0.1 M tetraethyl ammoniumtetrafluoroborate (Aldrich)/acetonitrile solution under argon.

Poly[3,4-ethylenedioxythiophene], PEDOT, was polymerized on ITO-glass from a solution of 0.1 M 3,4-ethylenedioxythiophene, EDOT (Bayer), in acetonitrile that contained 0.1 M LiClO₄/CH₃CN solution. The polymerization was carried out potentiostatically at 1.8 V (*vs.* Ag/AgCl quasi-reference electrode) for 2 seconds. The film formed was semi-transparent. The quasi-reference electrode was prepared by applying a voltage of 4.6 V from a dc source to an Ag wire dipped along with the counter platinum wire in a saturated aqueous solution of KCl.

Device preparation and characterizations

ITO-glass sheets, each of dimensions 1.5 cm x 2.5 cm were cleaned successively with deionized water, acetone and isopropyl alcohol and dried in air. Nanocrystalline TiO₂ films were formed by the hydrolysis of titanium isopropoxide according to the literature [20, 23]. Thus, 0.5 mL of titanium isopropoxide (Aldrich, 99 %) was slowly added with vigorous stirring to a mixture of 2.5 mL of glacial acetic acid (Sigma Aldrich), 7.5 mL of isopropanol (Sigma Aldrich) and 2.5 mL of deionized water under argon atmosphere. The solution was stirred for three days to obtain a viscous solution. The TiO₂ colloidal solution was applied on the surface of the ITO-glass and distributed with a glass rod sliding over an adhesive tape that covered the glass edges. The adhesive tape controlled the thickness of the TiO₂ film, which is in the range of few micrometers. A non-coated area (0.5 cm x 1.5 cm) was left for electrical contact. After drying in

air, the TiO_2 was sintered at $450\text{ }^\circ\text{C}$ for 30 min in a furnace (Carbolite, ELF 11/14B model, England) and then cooled slowly.

The photoelectrochemical cells consisted of the I_3^-/I^- redox couple (Iodolyte, Solaronix) sandwiched between the photoactive electrode and a PEDOT coated on ITO-glass counter electrode. The two electrodes were separated by a Teflon spacer to prevent shorting. The photoactive electrode consisted of electropolymerized PDHOPT on either ITO-glass or on TiO_2 coated ITO-glass. PDHOPT is dedoped to its neutral state at 0.4 V vs. Ag/AgCl quasi-reference electrode in a monomer free electrolyte solution and then rinsed with acetonitrile and dried in air. The device was sealed with TG-50 sealant (Solaronix). The PEC was then mounted in a sample holder inside a metal box having a $1\text{ cm} \times 1\text{ cm}$ light entrance window, which determined the illumination area. The schematic layout of the photoelectrochemical cells used and the structures of PEDOT and PDHOPT are depicted in Figure 1.

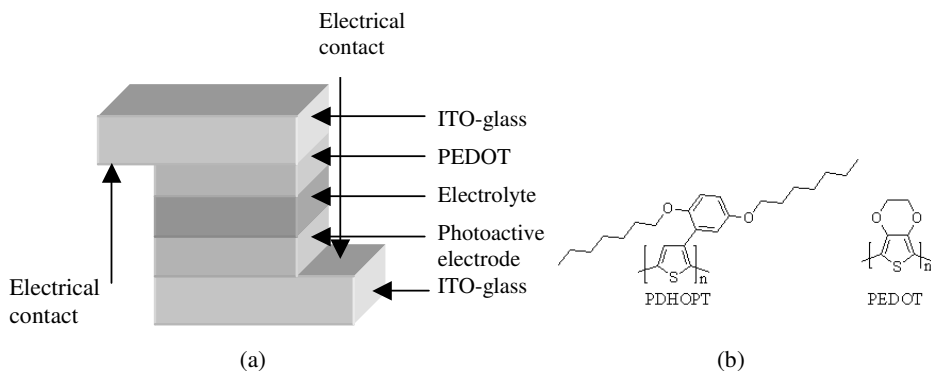


Figure 1. Schematic layout of (a) the photoelectrochemical cell used and (b) the structures of PDHOPT and PEDOT.

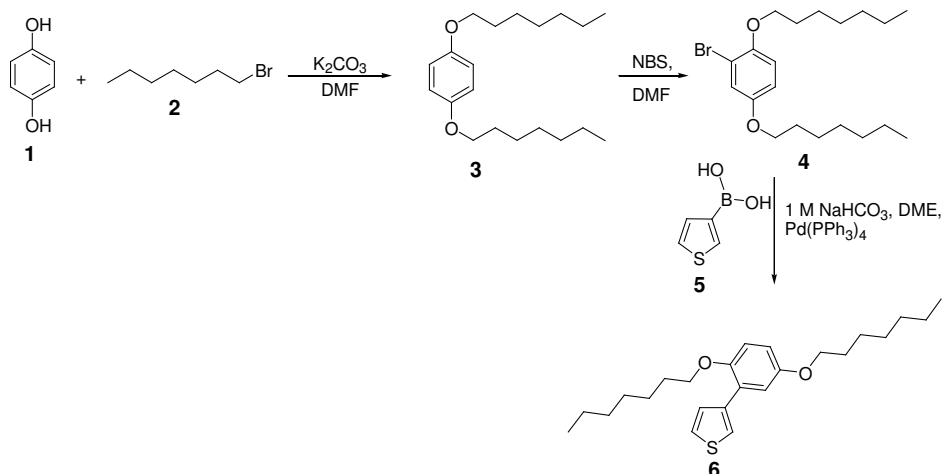
A 250 W tungsten-halogen lamp regulated by an Oriel power supply (Model 66182) was used to illuminate the PEC. For spectral studies, a grating monochromator (Model 77250) was used to select a wavelength manually between 300 nm and 800 nm at an interval of 10 nm. The steady-state current was recorded after illuminating the device for 60 seconds at each selected wavelength. All spectra were corrected for the spectral response of the lamp and the monochromator by normalization to the response of a calibrated silicon photodiode (Hamamatsu, model S-1336-8BK). The white light intensity was measured in the position of the sample cell with a Conrad electronic luxmeter (Model LX-101). For intensity dependence measurements a series of neutral density filters were placed between the light source and the sample holder to vary the light intensity incident on the sample. The electrochemical and the photoelectrochemical properties were studied using CHI600A Electrochemical Analyzer. Optical absorption measurements were carried out using a Perkin-Elmer Lambda 19 UV/VIS/NIR spectrometer.

RESULTS AND DISCUSSION

Synthesis of 3-(2',5'-diheptyloxyphenyl)thiophene (6)

Schemes 1 shows the reaction pathway that led to compound **6**. Thus, treatment of hydroquinone (**1**) with heptyl bromide (**2**) in the presence of K_2CO_3 in DMF gave 1,4-

diheptyloxybenzene (**3**). Bromination of compound **3** with NBS and DMF gave 1-bromo-2,5-diheptyloxy benzene (**4**), which was subsequently coupled with 3-thiopheneboronic acid (**5**) through a Pd(0)-catalyzed Suzuki [24] reaction to lead to 3-(2',5'-diheptyloxyphenyl)thiophene (**6**).



Scheme 1. Synthesis of 3-(2', 5'-diheptyloxyphenyl)thiophene (**6**).

Electrochemical synthesis and characterization of poly[3-(2',5'-diheptyloxyphenyl)-thiophene]

Figure 2 shows the cyclic voltammogram for the electrochemical polymerization of DHOPT on glassy carbon disk electrode. Oxidation of the monomer starts around 0.93 V with peak potential at 1.09 V. The oxidation of the monomer increases from cycle to cycle, giving more of its polymer film that gives peaks for oxidation (p-doping) and dedoping at 0.86 V. Upon continued cycles, the peak potentials shift slightly towards positive and negative directions, respectively, indicating a slightly slower kinetics for the electron transfer reactions with the deposition of more of the polymer. The polymerization on *nc*-TiO₂ coated ITO-glass takes place on the surface of the ITO and the film grows within the pores of the *nc*-TiO₂ film. The color of the polymer film changes between blue in its oxidized state and yellow in its neutral state. The polymer adheres strongly on TiO₂ coated ITO-glass and on glassy carbon, but slightly less on ITO-glass. Figure 3 shows the cyclic voltammogram of PDHOPT in a monomer free electrolyte solution that contains 0.1 M tetraethylammoniumtetrafluoroborate (TEATFB) in acetonitrile. The onset potential for the oxidation of PDHOPT is 0.86 V *vs.* Ag/AgCl. The HOMO level of the polymer is determined using the empirical equation proposed by Bredas *et al.* [25] by adding a value of 4.4 to the onset of oxidation measured against the Ag/AgCl reference electrode which is found to be $-(0.86 + 4.4) \approx -5.3$ eV. The optical band gap of the neutral polymer as determined from the onset of the UV-Vis absorption peak (580 nm) is 2.1 eV (Figure 4). Thus, The LUMO level of the polymer is estimated by subtracting the optical band gap from the HOMO level and is found to be -3.2 eV. These energy positions can allow the transfer of electrons from the excited state of the polymer to the conduction band edge of TiO₂ ($E_{CB(TiO_2)} = -4.2$ eV [26]) and the transfer of holes from the HOMO of the polymer to I₃⁻/I⁻ redox mediator whose redox potential is around -4.9 eV [2].

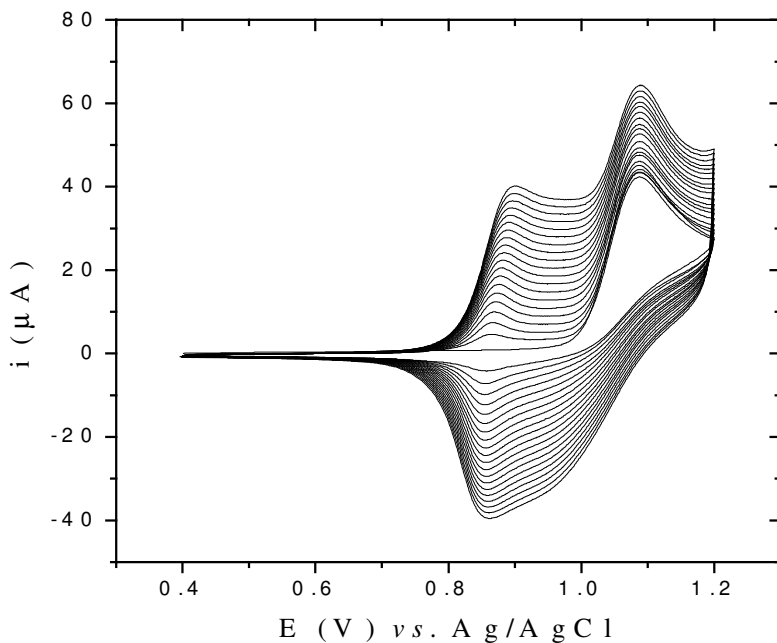


Figure 2. Cyclic voltammograms recorded for the electropolymerization of 1 mM DHOPT on glassy carbon disk electrode in CH_3CN solution containing 0.1 M of LiClO_4 . The potential is scanned repetitively between 0.4 V and 1.2 V at a scan rate of 10 mV/s.

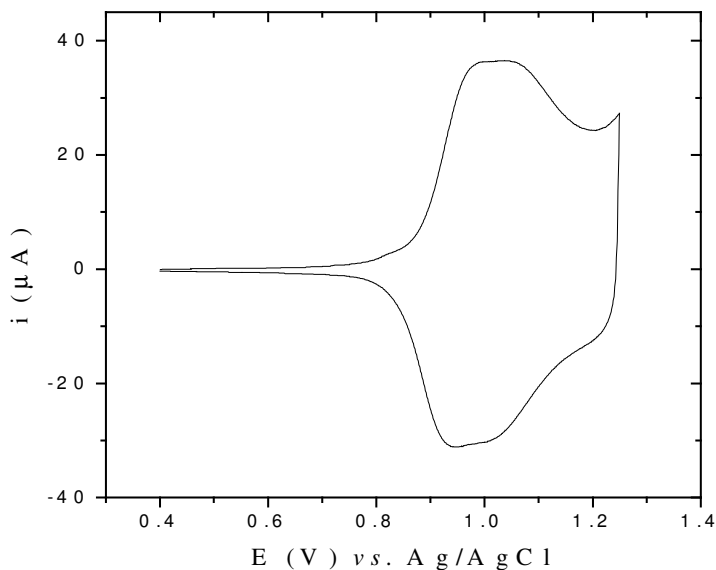


Figure 3. Cyclic voltammogram of PDHOPT on glassy carbon disk electrode recorded in a 0.1 M TEATFB/ CH_3CN solution at a scan rate of 10 mV/s.

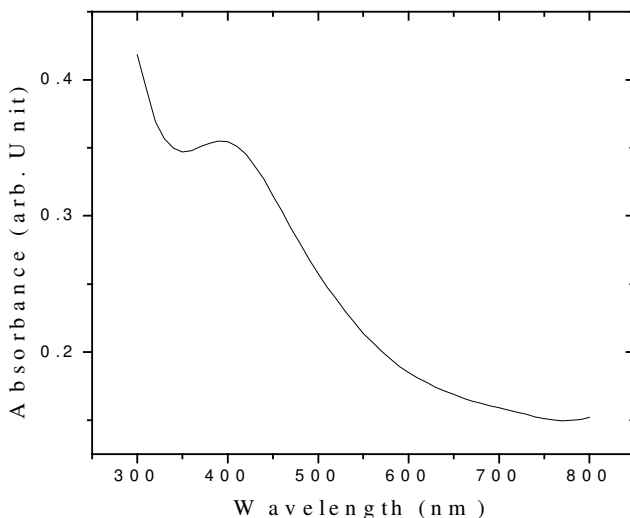


Figure 4. UV-Vis absorption spectra of the undoped PDHOPT film on ITO-glass.

The photoresponse behaviors of the photoelectrochemical cells

Figure 5 and Figure 6 show the current voltage curves of the photoelectrochemical devices, both in the dark and under white light illumination where the photoactive electrode consists of a film of PDHOPT and a composite film of PDHOPT/TiO₂, respectively. The photoelectrochemical characteristics of the devices are compared in Table 1. The device parameters, the fill factor (FF), the power conversion efficiency (η) and the induced photon-to-current conversion efficiency (IPCE) were calculated using the following equations [27]:

$$FF = \frac{I_p V_p}{I_{sc} V_{oc}} \quad (1)$$

$$\eta (\%) = \frac{FF I_{sc} (A/cm^2) V_{oc} (V)}{P_{in} (W/cm^2)} \times 100 \quad (2)$$

$$IPCE (\%) = \frac{1240 I_{sc} (\mu A/cm^2)}{\lambda (nm) I (W/m^2)} \quad (3)$$

where V_{oc} is the open-circuit voltage, I_{sc} is the short-circuit current, λ is the excitation wavelength, I is the monochromatic light intensity, P_{in} is the intensity of the white light and V_p and I_p are the voltage and the current at the maximum power point of the I-V curve.

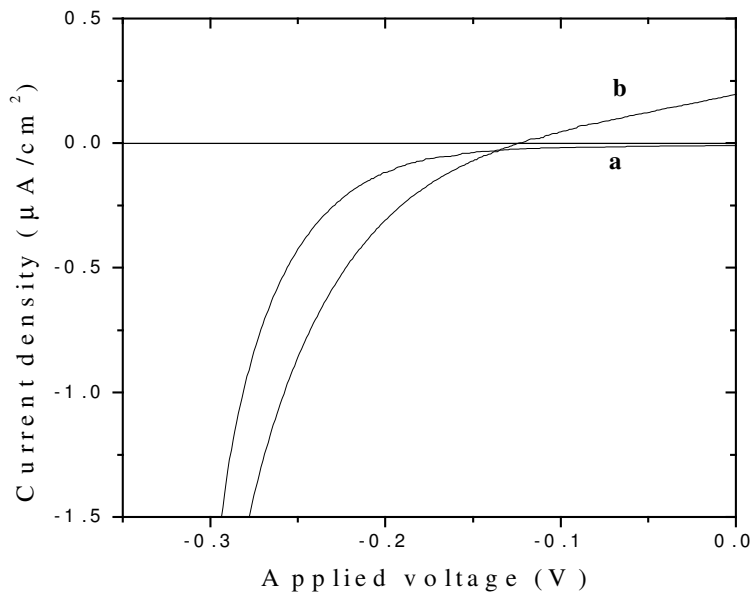


Figure 5. Current density vs. voltage characteristics of the PDHOPT based liquid-state PEC. **a**: In the dark, **b**: Under white light illumination from the ITO/PDHOPT side (backside) with light intensity of $80\text{ mW}/\text{cm}^2$.

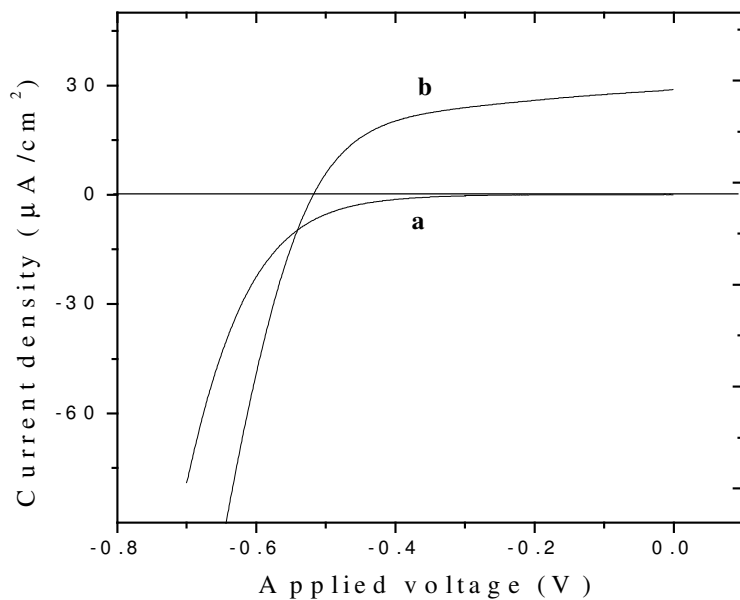


Figure 6. Current density vs. voltage characteristics of the $\text{nc-TiO}_2/\text{PDHOPT}$ based liquid-state PEC. **a**: In the dark, **b**: Under white light illumination from the ITO/ $\text{TiO}_2/\text{PDHOPT}$ side (backside) with light intensity of $80\text{ mW}/\text{cm}^2$.

Table 1. The performance of photoelectrochemical devices containing PDHOPT and TiO₂/PDHOPT as photoactive electrodes when illuminated with light intensity of 80 mW/cm².

Photoactive electrode	V _{OC} (mV)	I _{SC} (μA/cm ²)	FF	η (%) (x 10 ⁻³)
PDHOPT	125	0.2	0.27	0.84
TiO ₂ /PDHOPT	520	29	0.54	1018

Devices containing TiO₂/PDHOPT photoactive electrode exhibit higher V_{OC}, I_{SC} and FF when compared with devices containing PDHOPT only. Though the power conversion efficiencies of both types of devices are low, devices made from TiO₂/PDHOPT show improved performance by 3 orders of magnitude.

Figure 7 and Figure 8 show the incident photon-to-current conversion efficiencies (IPCE) of PDHOPT and TiO₂/PDHOPT based devices, respectively. When compared with PDHOPT based devices, the TiO₂/PDHOPT based devices have higher IPCE values at each wavelength.

The normalized photocurrent action spectra of PDHOPT and TiO₂ based devices along with the normalized absorption spectrum of PDHOPT are depicted in Figure 9. From the figure it can be observed that both types of devices follow similar pattern with the absorption spectrum of PDHOPT, PDHOPT based devices being closer.

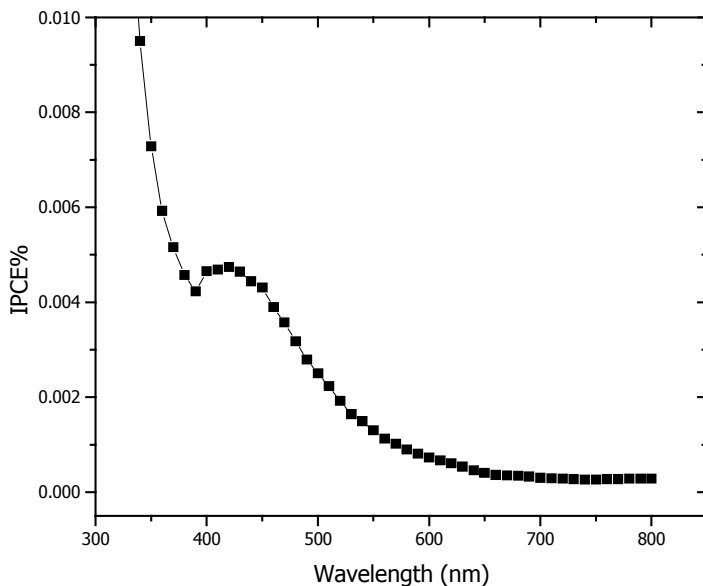


Figure 7. Short-circuit photocurrent action spectrum of PDHOPT based liquid-state PEC under illumination from the front side.

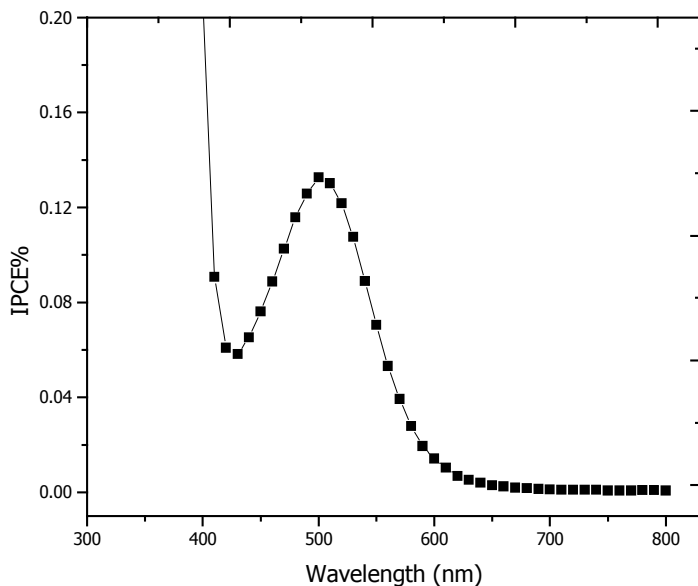


Figure 8. Short-circuit photocurrent action spectrum of $nc\text{-TiO}_2/\text{PDHOPT}$ based liquid-state PEC under illumination from the front side.

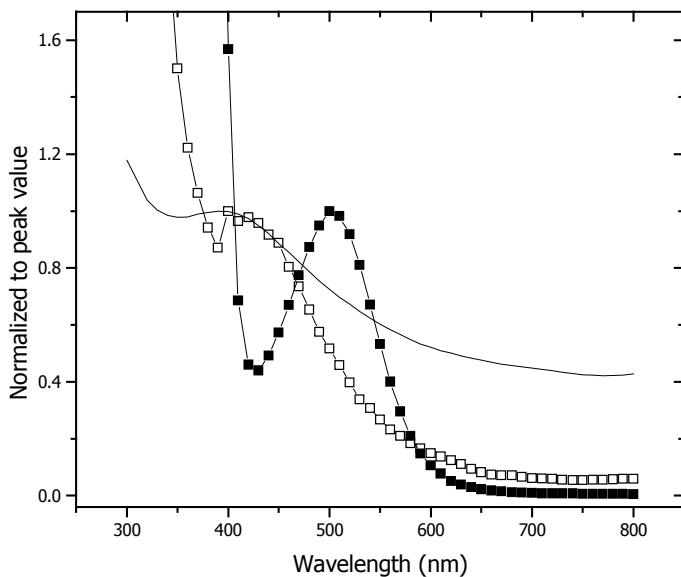


Figure 9. Normalized optical absorption spectrum of PDHOPT (solid line) and normalized photocurrent action spectrum of PDHOPT based (open squares) and $\text{TiO}_2/\text{PDHOPT}$ based (closed squares) devices for front side illuminations.

The dependence of V_{OC} and I_{SC} on incident light intensity for PDHOPT and TiO_2 /PDHOPT based devices are shown in Figures 10 and 11, respectively. From the figures it can be observed that the V_{OC} and the I_{SC} are more dependent on light intensity in devices that contain TiO_2 /PDHOPT photoactive electrode indicating better charge separation in the devices. In Figure 11, the photocurrent for PDHOPT based devices increases less rapidly than the first power (an ideal value) of the light intensity (slope = 0.86), indicating the presence of exciton recombination due to surface states that act as recombination centers. For TiO_2 /PDHOPT based device, the photocurrent increases more rapidly than the first power of the light intensity (slope = 1.3), indicating an increase in the lifetime of the free charge carriers with their increasing density [28].

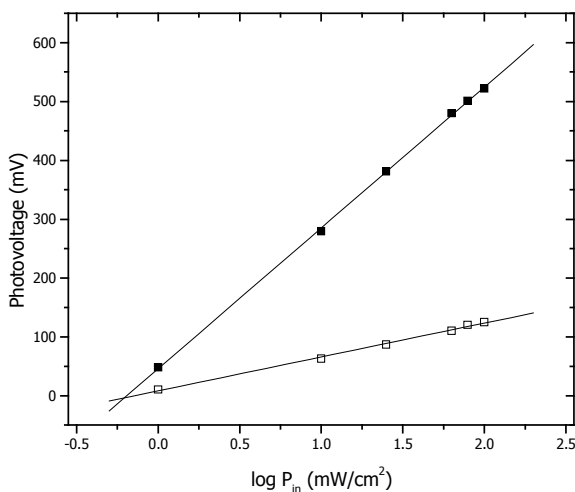


Figure 10. Plot of V_{OC} vs. $\log P_{in}$ of PDHOPT based (open squares) and $nc-TiO_2$ /DHOPT based (closed squares) liquid-state PECs.

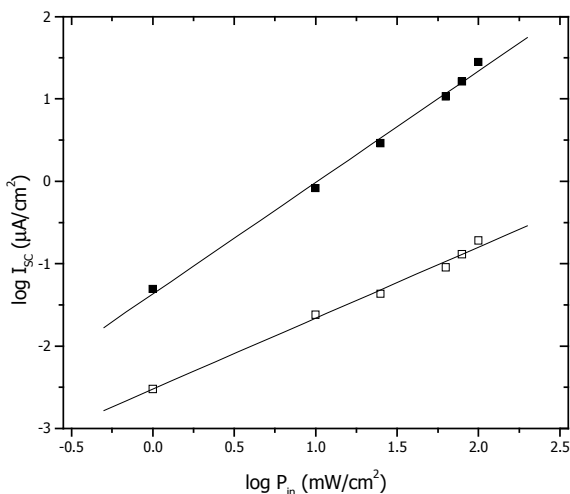


Figure 11. Plot of $\log I_{SC}$ vs. $\log P_{in}$ of PDHOPT based (open squares) and $nc-TiO_2$ /PDHOPT based (closed squares) liquid-state PECs.

CONCLUSIONS

The polymer, poly[3-(2',5'-diheptyloxyphenyl)thiophene], PDHOPT, has been prepared for the first time electrochemically from its monomer and used for solar cell application. The estimated energy levels of the highest occupied molecular orbital (HOMO) and the lowest unoccupied molecular orbital (LUMO) of PDHOPT are -5.3 eV and -3.2 eV, respectively. PDHOPT sensitizes nanocrystalline titanium dioxide in liquid-state photoelectrochemical cells. Devices where the photoactive electrode consists of nc-TiO₂/PDHOPT composite film showed improved cell performance over those that consist of PDHOPT alone. It has been observed that the V_{OC} and the I_{SC} are more dependent on light intensity in devices that contain TiO₂/PDHOPT photoactive electrode indicating better charge separation in the devices with increasing light intensities.

ACKNOWLEDGEMENTS

The authors thank the Ethiopian Science and Technology commission, the Third World Academy of Sciences, Trieste, Italy and SIDA/SAREC for financial support. The authors gratefully thank Prof. N.S. Sariciftci, Linz Institute for Organic Solar Cells, for providing chemicals.

REFERENCES

1. O'Regan, B.; Grätzel, M. *Nature* **1991**, 353, 737.
2. Hagfeldt, A.; Grätzel, M. *Acc. Chem. Res.* **2000**, 33, 269.
3. Hirsch, A.; Kroon, J.M.; Kern, R.; Uhlendorf, I.; Holzbock, J.; Meyer, A.; Ferber, J.A. *Prog. Photovolt: Res. Appl.* **2001**, 9, 425.
4. Grünwald, R.; Tributsch, H. *J. Phys. Chem. B* **1997**, 101, 2564.
5. Nogueira, A.F.; Durrant, J.R.; De Paoli, M.A. *Adv. Mater.* **2001**, 13, 826.
6. Kubo, W.; Kambe, S.; Nakade, S.; Kitamura, T.; Hanabusa, K.; Wada, Y.; Yanagida, S. *J. Phys. Chem. B* **2003**, 107, 4374.
7. Stathatos, E.; Lianos, P.; Jovanovski, V.; Oriol, B. *J. Photochem. Photobio. A: Chemistry* **2005**, 169, 57.
8. Hao, Y.; Yang, M.; Yu, C.; Cai, S.; Liu, M.; Fan, L.; Li, Y. *Solar Energy Mater. Solar Cells* **1998**, 56, 75.
9. Van Hall, P.A.; Wienk, M.M.; Kroon, J.M.; Verhees, W.J.H.; Slooff, L.H.; van Gennip, W.J.H.; Jonkheijm, P.; Janssen, R.A.J. *Adv. Mater.* **2003**, 15, 118.
10. Senadeera, G.K.R.; Kitamura, T.; Wada, Y.; Yanagida, S. *Solar Energy Mater. Solar Cells* **2005**, 88, 315.
11. Li, G.; Shrotriya, V.; Huang, J.; Yao, Y.; Moriarty, T.; Emery, K.; Yang, Y. *Nature* **2005**, 4, 864.
12. Reyes-Reyes, M.; Kim, K.; Carroll, D.L. *Appl. Phys. Lett.* **2005**, 87, 083506.
13. Ma, W.; Yang, C.; Gong, X.; Lee, K.; Heeger, A.J. *Adv. Funct. Mater.* **2005**, 15, 1617.
14. Arango, A.C.; Johnson, L.; Horhold, H.; Schlesinger, Z.; Carter, S.A. *Adv. Mater.* **2000**, 12, 1689.
15. Gebeyehu, D.; Brabec, C.J.; Padinger, F.; Fromherz, T.; Spiekermann, S.; Vlachopoulos, N.; Kienberger, F.; Schindler, H.; Sariciftci, N.S. *Synth. Met.* **2001**, 121, 1549.
16. Huynh, W.U.; Dittmer, J.J.; Alivisatos, A.P. *Science* **2002**, 295, 2425.
17. Smestad, G.P.; Spiekermann, S.; Kowalik, J.; Grant, C.D.; Schwartzberg, A.M.; Zhang, J.; Tolbert, L.M.; Moons, E. *Solar Energy Mater. Solar Cells* **2003**, 76, 85.

18. Arici, E.; Hoppe, H.; Schäffler, F.; Meissner, D.; Malik, M.A.; Sariciftci, N.S. *Thin Solid Films* **2004**, 451-452, 612.
19. Beck, W.J.E.; Wienk, M.M.; Janssen, R.A.J. *Adv. Mater.* **2004**, 16, 1009.
20. Grant, C.D.; Schwartzberg, A.M.; Smestad, G.P.; Kowalik, J.; Tolbert, L.M.; Zhang, J.Z. *J. Electroanal. Chem.* **2002**, 522, 40.
21. Yohannes, T.; Inganäs, O., *Solar Energy Mater. Solar Cells* **1998**, 51, 93.
22. Andersson, M.R.; Mammo, W.; Olinga, T.; Svensson, M.; Theander, M.; Inganäs, O. *Synth. Met.* **1999**, 101, 11.
23. Tennakone, K.; Kumara, G.R.R.A.; Kottegoda, I.R.M.; Wijayantha, K.G.U.; Perera, V.P.S. *J. Phys. D: Appl. Phys.* **1998**, 31, 1492.
24. Miyaura, N.; Yanagi, T.; Suzuki, A. *Synth. Commun.* **1981**, 11, 513.
25. Bredas, J.L.; Silbey, R.; Boudreaux, D.S.; Chance, R.R. *J. Am. Chem. Soc.* **1983**, 105, 6555.
26. Xu, Y.; Schoonen, M.A.A. *American Mineralogist* **2000**, 85, 543.
27. Karlin, K.D. *Progress in Inorganic Chemistry*, Vol. 41, John Wiley and Sons: California; **1994**; p 81.
28. Hyde, F.J. *Semiconductors*, Macdonald & Co. (Publishers) Ltd.: London, **1965**; p 227.